

YMTHE, Volume 31

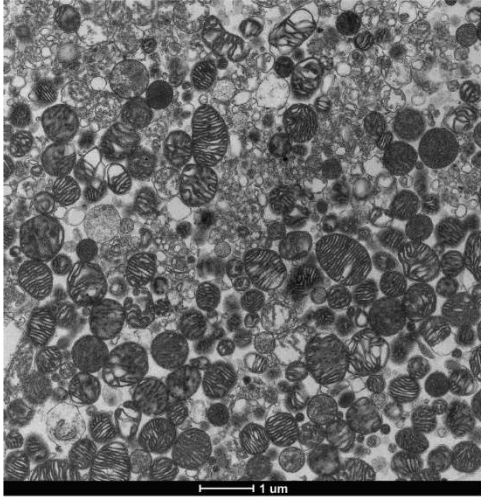
Supplemental Information

**Delivery of mitochondria confers
cardioprotection through mitochondria
replenishment and metabolic compliance**

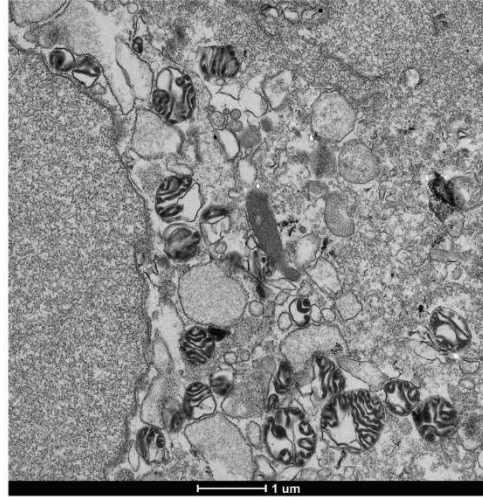
Alian Zhang, Yangyang Liu, Jianan Pan, Francesca Pontanari, Andrew Chia-Hao Chang, Honghui Wang, Shuang Gao, Changqian Wang, and Alex CY. Chang

Table S1. GO analysis of 804 atrial and 1192 ventricular mitochondrial transplantation perturbed genes.

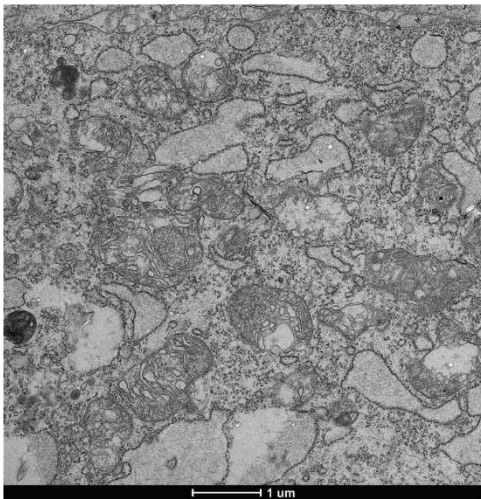
Table S2. RT-qPCR primers used.



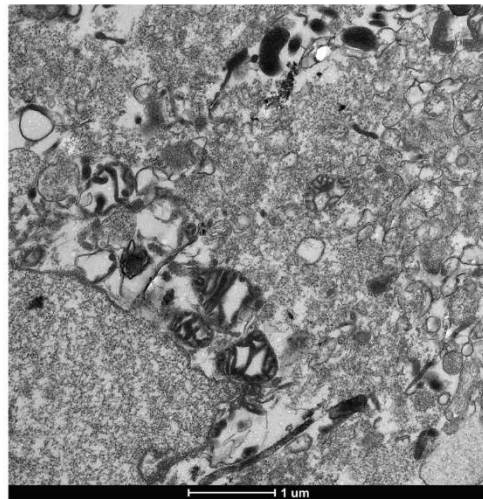
Modified Preble *et al.*
J. Vis. Exp. 2014



Frezza *et al.*
Nature Protocols 2007



Thermo Mitochondrial
Isolation Kit (Cat. No. 89874)



Wieckowski *et al.*
Nature Protocols 2009

Figure S1. Evaluation of mitochondria ultrastructure by transmission electron microscopy.

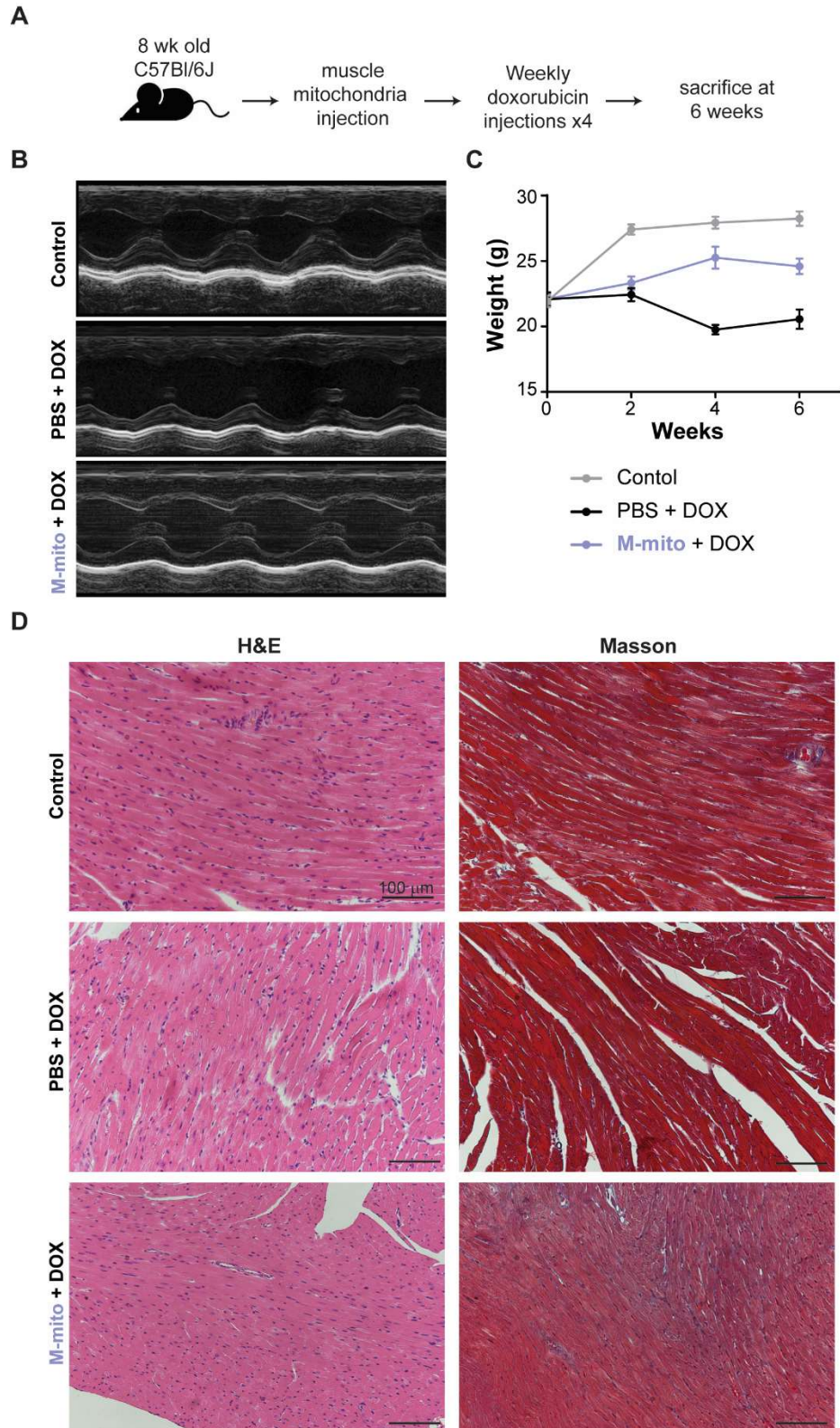


Figure S2. Doxorubicin heart failure model. (A) Schematic of doxorubicin heart failure mouse model. (B) Representative left ventricular M-mode echocardiographic and pulsed-wave Doppler tracings. (C) Animal weight during doxorubicin challenge (N = 6 animals per group). Data are shown as mean \pm SEM. (D) Representative images of H&E and Masson staining.

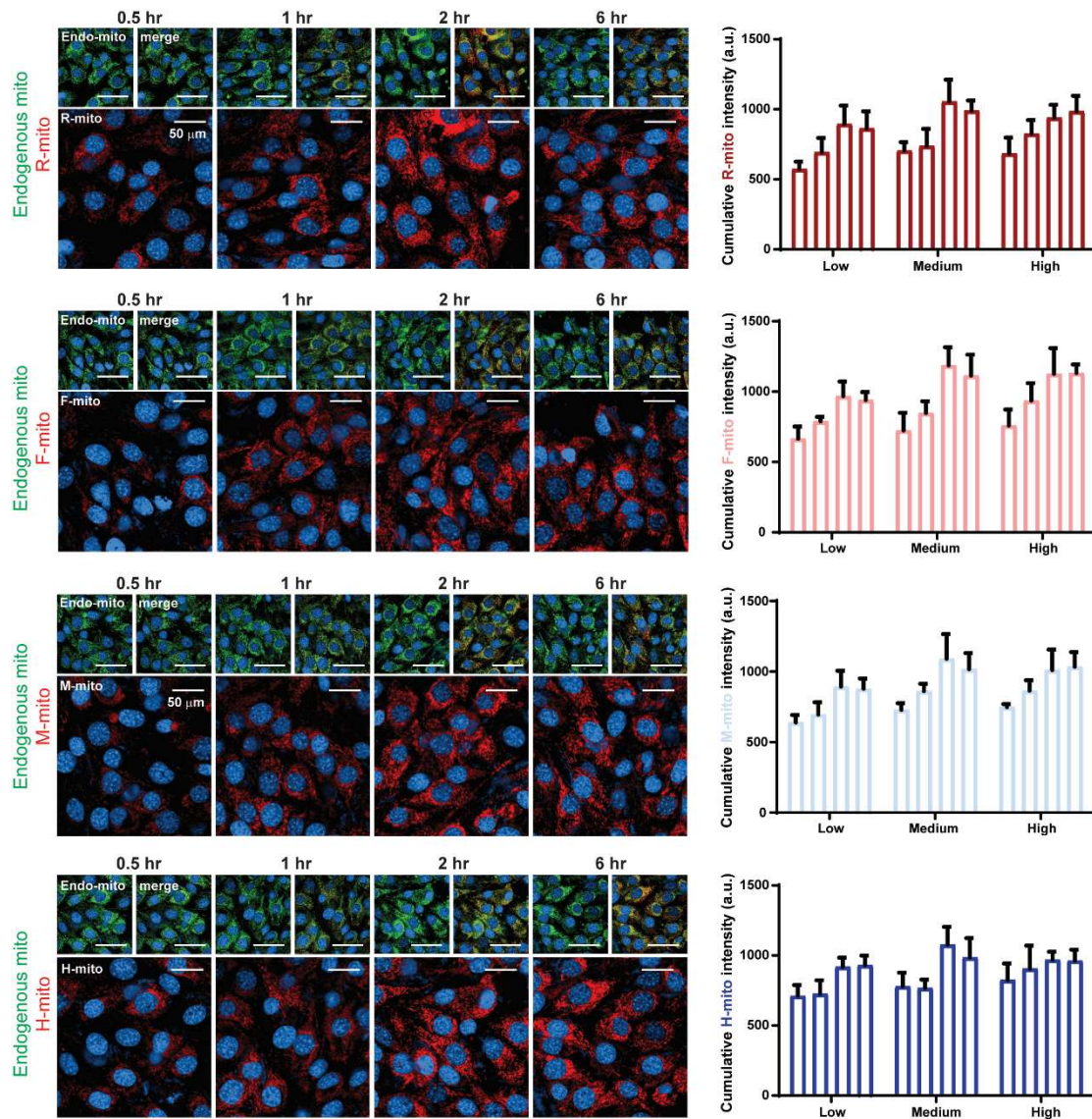


Figure S3. Mitochondria absorption kinetics of neonatal murine ventricular cardiomyocytes. Representative cardiomyocyte micrographs are shown. Cumulative R-mito, F-mito, M-mito and H-mito signals at 0.5h, 1h, 2h, and 6h are shown (N = 20-25 neonatal hearts were pooled for NMVM isolation; n = 3). Three mitochondrial concentrations were tested (low: $0.5 \times 10^4/100\mu\text{L}$; medium: $1.0 \times 10^4/100\mu\text{L}$; high: $2.0 \times 10^4/100\mu\text{L}$). Data are shown as mean \pm SEM.

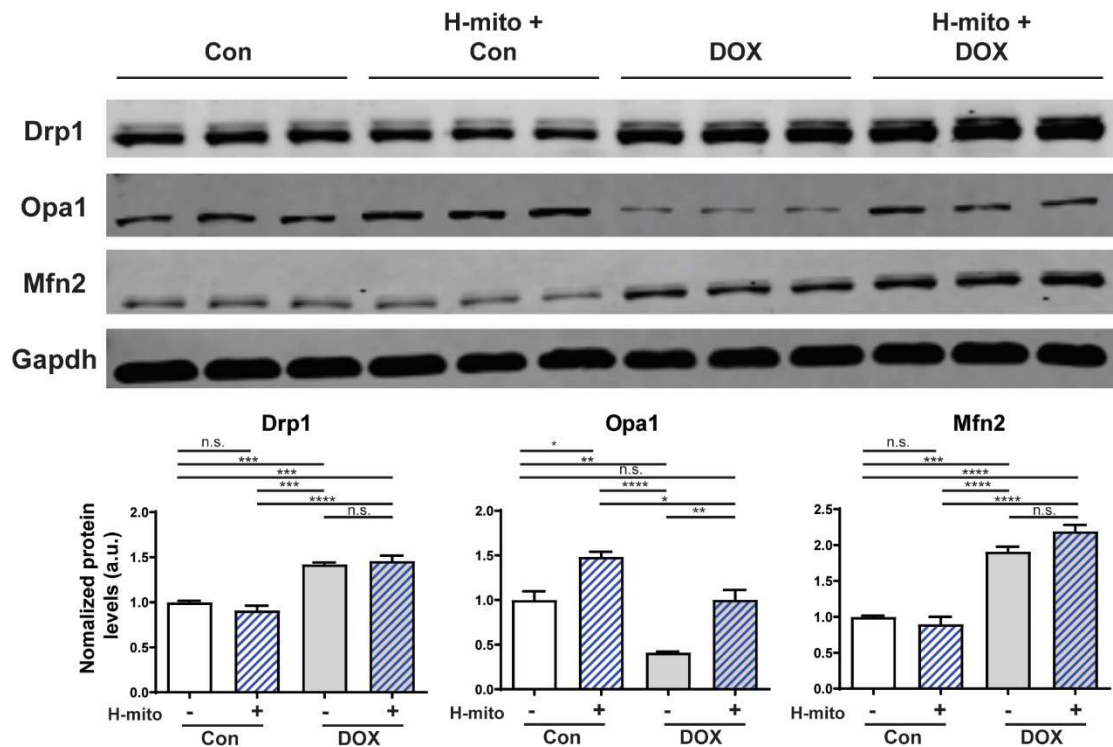


Figure S4. Mitochondria transplantation and doxorubicin treatment alters mitochondrial homeostasis. Cardiomyocytes isolated from animals treated with or without H-mito and challenged with or without doxorubicin were immunoblotted for mitofusion Opa1 and Mfn2 and mitofission Drp1 protein (N = 3 animals each). Gapdh expression was used as loading control and quantifications are shown. Data are shown as mean \pm SEM. Significance was determined by one-way ANOVA. *P<0.05, **P<0.01, ***P<0.001, ****P<0.0001.

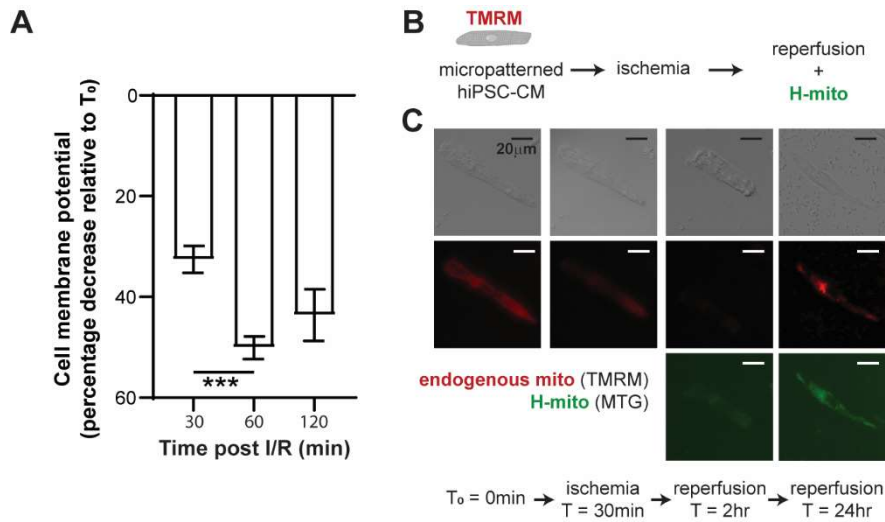


Figure S5. Evaluation of mitochondrial membrane potential during ischemia reperfusion. (A) Ischemic reperfusion challenge in healthy hiPSC-CMs results in loss of mitochondrial membrane potential ($n = 15\text{-}37$ cells). Data are shown as mean \pm SEM. Significance was determined by one-way ANOVA for the remaining panels. $***P < 0.001$. (B-C) Live cell microscopy demonstrating restoration of mitochondrial membrane potential in cardiomyocytes challenged by ischemia reperfusion by transplanting mitochondria isolated from healthy hiPSC-CMs.

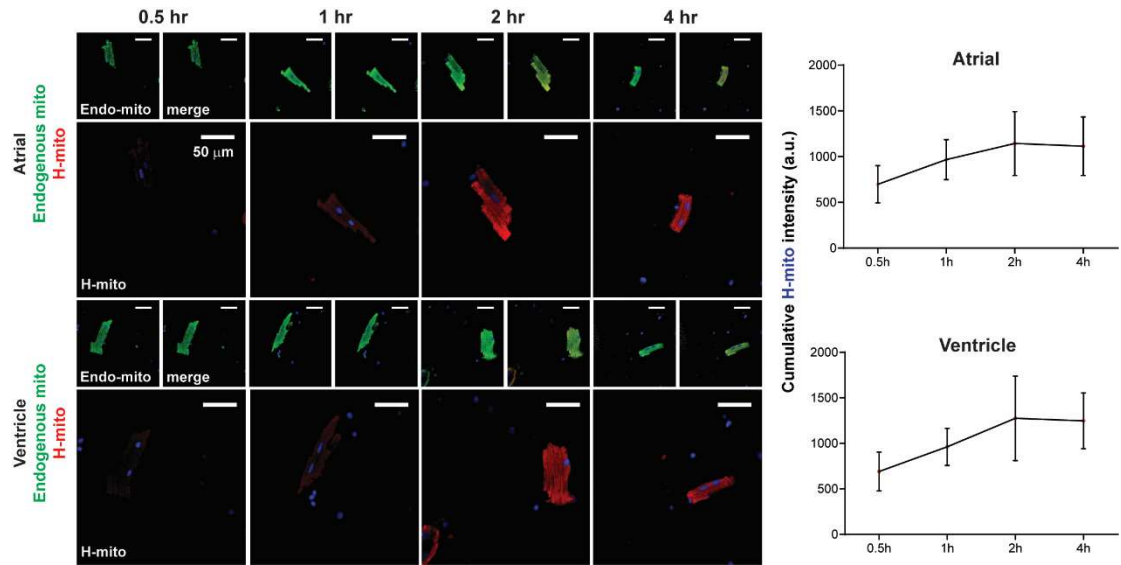


Figure S6. Mitochondria absorption kinetics of Langendorff purified atrial and ventricular murine cardiomyocytes. Representative atrial and ventricular cardiomyocyte micrographs are shown. Cumulative H-mito signal over time are shown (N = 3 animals each). Data are shown as mean \pm SEM.